Chemical vapour deposition of Ca(Ti, Fe)O₃ thin film by thermal decomposition of organocomplexes

H. ITOH, I. OIKAWA, H. IWAHARA
Synthetic Crystal Research Laboratory, School of Engineering, Nagoya University, Chikusa-ku, Nagoya 464-01, Japan

M. AIZAWA
R and D Division, Toto Ltd, 2-8-1 Chigasaki-shi, Kanagawa 253, Japan

A thin film of Ca(Ti, Fe)O₃, which is a mixed conductor of oxide ions and electrons, was prepared on various substrates by chemical vapour deposition using organocomplexes $Ca(C_{11}H_{19}O_2)_2$, $Ti(O{-}^{i}C_3H_7)_4$ and $Fe(C_5H_7O_2)_3$ as starting materials. These complexes were evaporated at temperatures of 250, 115 and 45 °C, respectively, and transported to the substrate surface at an almost steady state. Homogeneous films of single-phase Ca(Ti, Fe)O₃ were obtained at deposition temperatures of 750–800 °C under the total pressure of 30 torr for the reaction time of 60–90 min on silica glass substrate. The amount of Ca(Ti, Fe)₃ films formed and their microstructure were found to be greatly affected by the compositions and surface structures of substrate materials.

1. Introduction

$CaTi_{1-x}Fe_xO_{1-\alpha}$ ($x \sim 0.2$), which possesses a substituted perovskite-type structure for $CaTiO_3$, is known as a mixed conductor of both oxide ions and electrons at elevated temperatures [1]. The oxide ion conductivity is $10^{-2}–10^{-1}$ S cm^{-1} and the oxide ion transport number is about 0.5–0.6 in air at 700–1000 °C. Such a mixed conductor would be applied to an electrochemical extractor for oxygen [2] or a diaphragm for hydrogen production [3] which requires neither electrode nor an external connecting lead. The extraction rate of oxygen from air, for example, was verified by Iwahara *et al.* [2] to exceed that of a conventional silicone film in using $CaTi_{0.8}Fe_{0.2}O_{3-\alpha}$ sintered ceramics. It is essential, however, for actual application to an oxygen extractor, to decrease the total oxide ion resistance of the whole mixed conductor. An appropriate assembly for such an extractor would be fabricated, if a dense thin film of the mixed conductor were formed on any porous susceptor.

Chemical vapour deposition (CVD) by a thermal decomposition of organocomplexes is one of the promising procedures to prepare such a multi-component oxide film on a porous substrate. Many perovskite-type oxide films such as dielectrics [4–8] or superconductors [9–11] have been prepared by CVD using organometallic compounds, alkoxides or β-diketonates as starting materials. However, the preparation of calcium titanate thin film by CVD has not been reported. In the present work, calcium dipivaloylmethanate $Ca(DPM)_2$ or $Ca(C_{11}H_{19}O_2)_2$, titanium isopropoxide $Ti(O{-}^{i}C_3H_7)_4$ and iron acetyl-acetonate $Fe(acac)_3$ or $Fe(C_5H_7O_2)_3$, were chosen as starting materials considering the stability and volatility of these organocomplexes. As a basic research on the CVD process in this system, the optimum conditions for obtaining the Ca(Ti, Fe)O₃ film were explored using silica glass substrate. The amount formed and the microstructure of the film on various substrates were also investigated under the optimum CVD conditions.

2. Experimental procedure

Fig. 1 shows the experimental equipment for preparation of Ca(Ti, Fe)O₃ film. In a horizontal quartz reaction tube (inside diameter 35 mm), two alumina boats were placed in the centres of the furnaces 1a and 2b, the temperatures of which were regulated independently. Given amounts of commercial powders $Fe(acac)_3$ and $Ca(DPM)_2$ were charged in the two boats, respectively. The vapours of these complexes were carried with a given flow of nitrogen gas. On the other hand, a liquid starting material of $Ti(O{-}C_3H_7)_4$ was evaporated at 45 °C using nitrogen carrier gas and then mixed with oxygen reactant gas. The mixed stream was introduced into the inlet between the evaporation furnace 1b and the deposition furnace 2. The substrates, such as silica glass, CVD–(TiO_2, CaO or Fe)/silica glass, and sintered Al_2O_3 or ZrO_2, were mounted vertically in furnace 2, as shown in Fig. 1. Both evaporation and deposition were performed under a constant reduced pressure in this uniaxial reactor tube. The specimens after CVD runs were annealed at 1000 °C for 60 min in air for stabilization
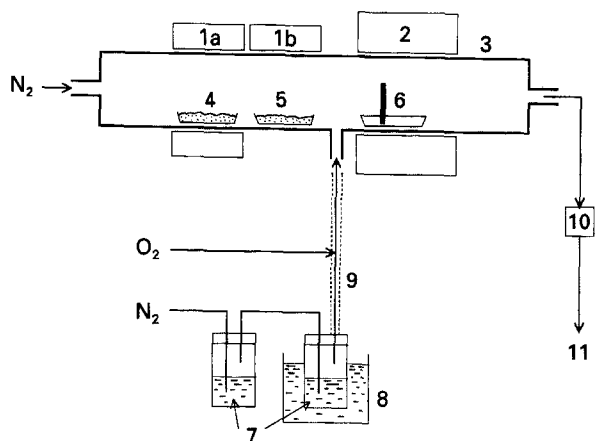
Figure 1 Experimental equipment for the preparation of Ca(Ti, Fe)O₃ film. 1a and b, evaporation furnaces; 2, deposition furnace; 3, quartz reactor tube; 4, Fe(C₅H₇O₂)₃; 5, Ca(C₁₁H₁₉O₂)₂; 6, substrate; 7, Ti(O–C₃H₇)₄; 8, oil bath; 9, tape heater; 10, cold trap; 11, vacuum pump.

of the deposited film. The evaporation behaviour of solid organocomplexes was examined by differential thermal analysis (DTA) and thermogravimetric analysis (TGA). The deposited specimen was identified by X-ray diffraction (XRD) and X-ray microanalysis (XMA). The microstructure of the film was observed by scanning electron microscopy (SEM).

3. Results and discussion

3.1. Evaporation and transport of organocomplexes

A supply of organocomplexes to the substrate surface in a steady state is important to enhance the reproducibility of thermal decomposition CVD experiments. Prior to deposition experiments, the evaporation behaviour of each complex was examined by DTA and TGA. In addition, a stable transport of the complex to the substrate surface was confirmed by measurement of the weight of deposited CaO, Fe₂O₃ or TiO₂ on the silica glass substrate. Fig. 2 shows the weight of deposited CaO as a function of evaporation temperature of Ca(DPM)₂ under the constant conditions of total pressure 40 torr (1torr = 133.322 Pa), flow rates of nitrogen 124 ml min⁻¹, and oxygen 30 ml min⁻¹, deposition temperature 900 °C, and reaction time 60 min. The maximum weight of deposit was obtained at the evaporation temperature of 240 °C. It was observed by DTA and TGA that Ca(DPM)₂ began to sublime at 150 °C, melted at 190 °C and burned out at 300 °C in air. On the other hand, Fe(acac)₃ gradually sublimed above 110 °C and burned out at 180 °C. The maximum weight of deposited Fe₂O₃ was observed at an evaporation temperature of 160 °C under the same deposition conditions as for Ca(DPM)₂. In order to depress the excess deposition of Fe₂O₃, it was necessary to decrease the evaporation temperature to below 140 °C. Fig. 3 shows the relation between the weight of deposited TiO₂ and the nitrogen carrier gas flow rate for the evaporation of Ti(O–C₃H₇)₄ under constant conditions: oxygen flow rate 30 ml min⁻¹,
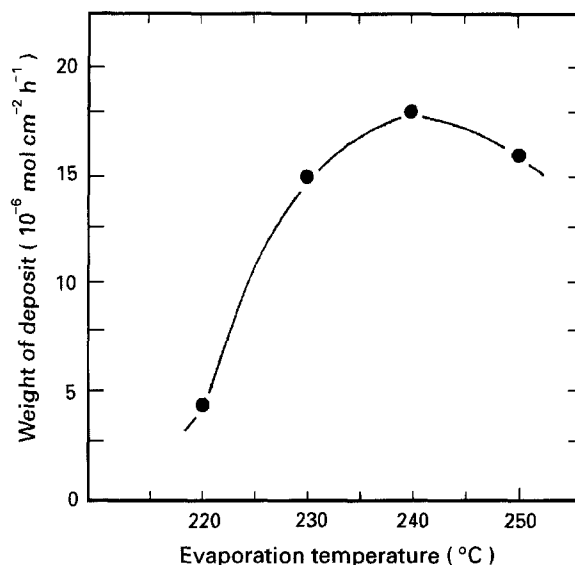

Figure 2 Weight of CaO deposited plotted against evaporation temperature of Ca(DPM)₂. Total pressure 40 torr; flow rates of nitrogen, 124 ml min⁻¹, and oxygen 30 ml min⁻¹; deposition temperature 900 °C, reaction time 60 min.
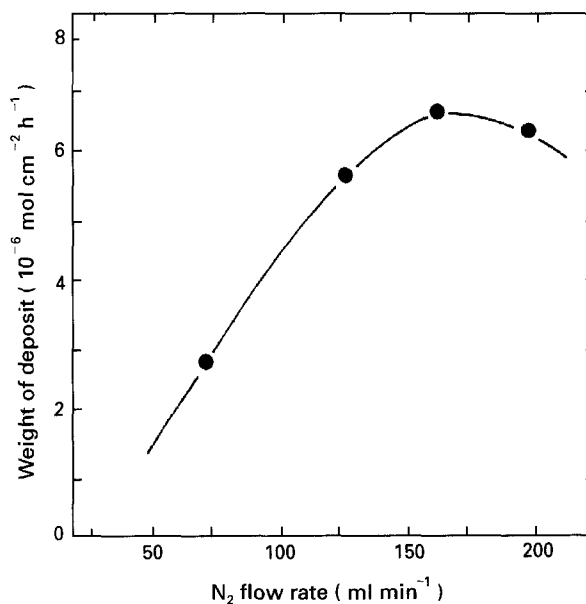

Figure 3 Weight of TiO₂ deposited plotted against nitrogen carrier gas flow rate for Ti(O–C₃H₇)₄. Total pressure 40 torr, oxygen flow rate 30 ml min⁻¹, deposition temperature 900 °C, reaction time 60 min, and evaporation temperature 45 °C.
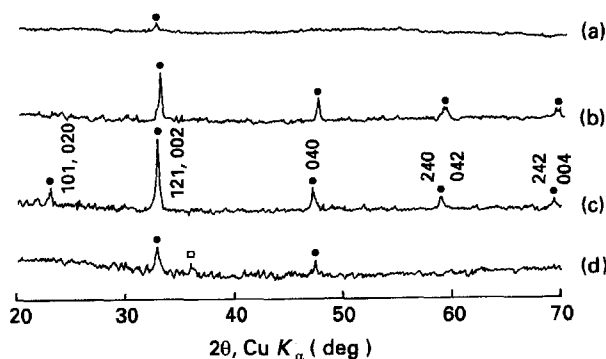

Figure 4 XRD patterns of the deposits on silica glass substrates at various deposition temperatures: (a) 650 °C, (b) 750 °C, (c) 800 °C and (d) 900 °C; reaction time 60 min. (●) Ca(Ti, Fe)O₃, (□) Fe₂O₃ (haematite).

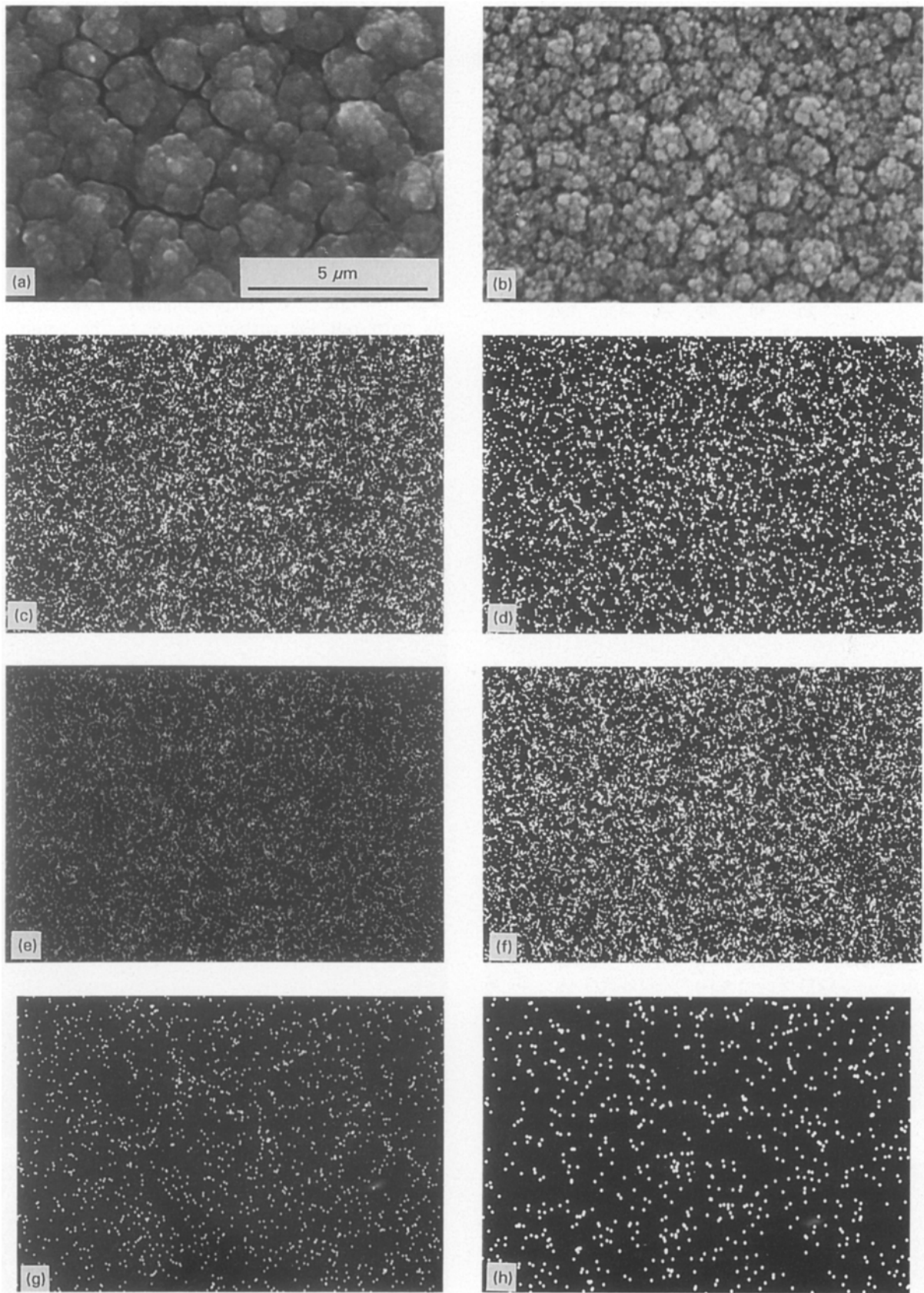*Figure 5* Surface appearances (a, b) and XMA images for (c, d) calcium, (e, f) titanium and (g, h) iron, in $Ca(Ti, Fe)O_3$ film on a silica glass substrate. Deposition temperatures (a, c, e, g) 750 °C, (b, d, f, h) 800 °C; reaction time 60 min.

deposition temperature 900 °C, reaction time 60 min, and evaporation temperature 45 °C. The amount of TiO_2 formed was found to be controlled by the nitrogen carrier gas flow rate up to 160 ml min^{-1}.

3.2. Optimum conditions for preparation of $Ca(Ti, Fe)O_3$ film

From the above data on evaporation and transport of each organocomplex, the evaporation temperatures of

2141

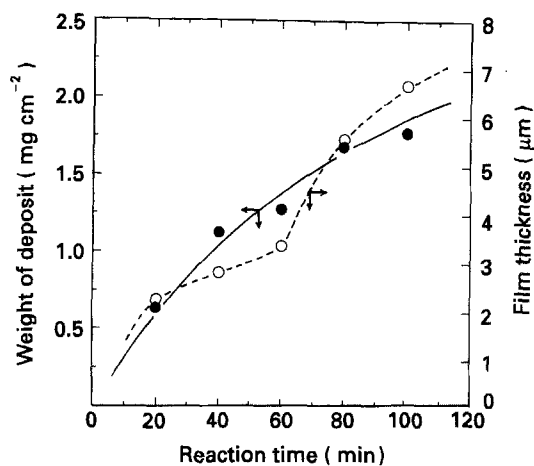*Figure 6* Weight deposited and film thickness of Ca(Ti, Fe)O$_3$ plotted against reaction time. Deposition temperature 750 °C, silica glass substrate.

Ca(DPM)$_2$, Fe(acac)$_3$ and Ti(O-C$_3$H$_7$)$_4$ were determined as 245, 115 and 45 °C, respectively. Because the influence of nitrogen carrier gas flow rate on the transport of calcium and iron sources was minor, the flow rate was kept constant at an appropriate value of 125 ml min^{-1} in all the subsequent experiments. The nitrogen carrier gas flow rate for transport of the titanium source was chosen as 195 ml min^{-1}. It was necessary to heat the tubing path to about 75 °C using a tape heater from the titanium source to the reactor, in order to prevent condensation of the alkoxide on the tube wall. A comparatively high flow rate of oxygen (100 ml min^{-1}) was streamed to burn out the carbon source in the complexes completely. The optimum conditions for deposition of Ca(Ti, Fe)O$_3$ films are summarized in Table I.

The influences of deposition temperature and reaction time were investigated in detail using silica glass substrate. Fig. 4 shows the variation in XRD patterns of the products deposited on silica glass substrate with

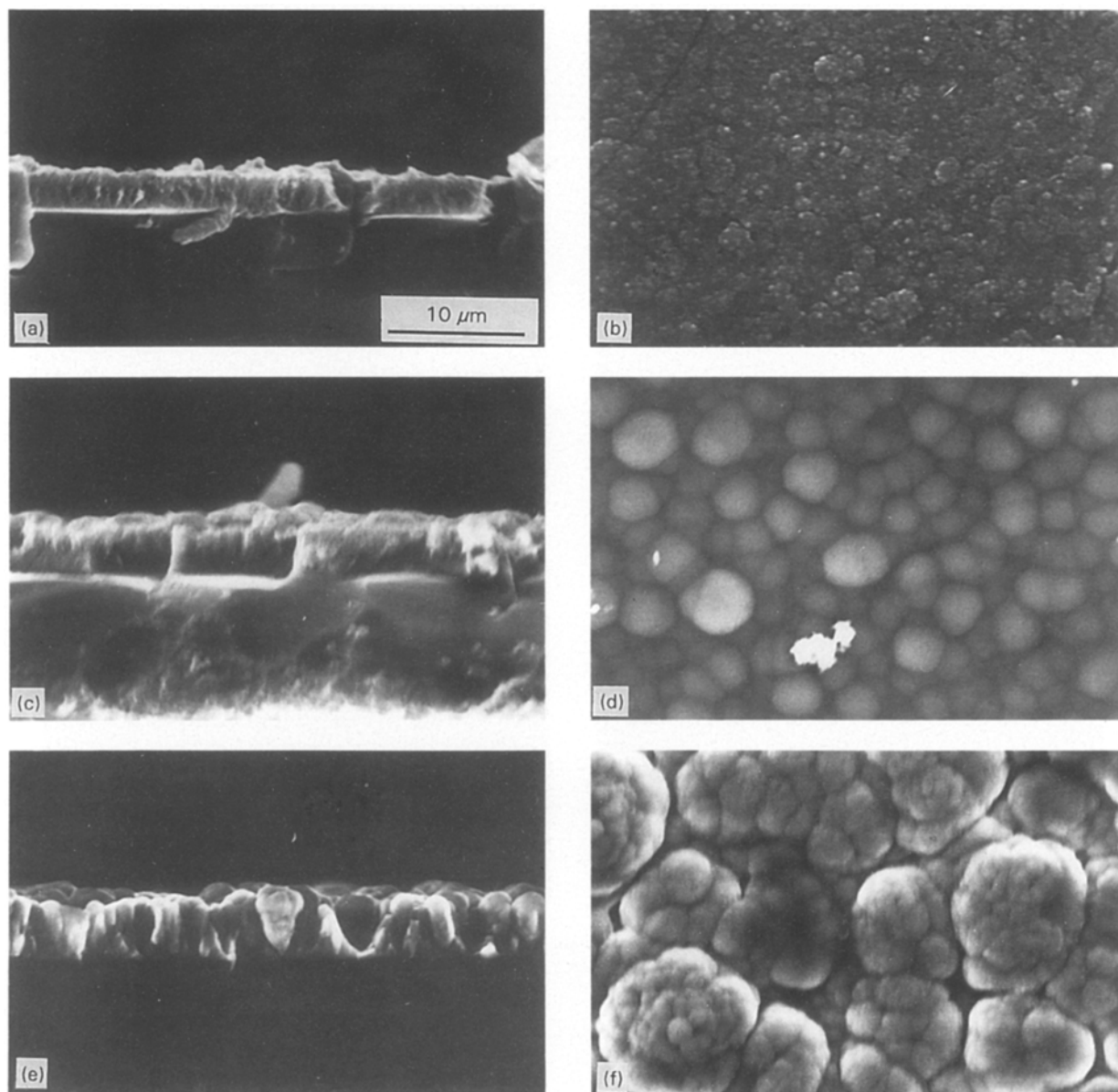*Figure 7* Scanning electron micrographs of cross-sections and surfaces of Ca(Ti, Fe)O$_3$ films obtained at various reaction times: (a, b) 20 min, (c) 40 min, (d) 60 min, (e) 80 min, (f) 100 min. Film thickness (a, b) 2.2 μm, (c) 4.0 μm, (d) 3.3 μm, (3) 5.6 μm, (f) 6.7 μm. Deposition temperature 750 °C, silica glass substrate.

2142

Evaporation temperature:	Ca(DPM)₂ 245 °C
	Fe(acac)₃ 115 °C
	Ti(O–C₃H₇)₄ 45 °C
Flow rate:	N₂ (total) 320 ml min⁻¹
	O₂ 100 ml min⁻¹
Total pressure:	30 torr
Deposition temperature:	700–800 °C
Reaction time:	20–60 min

deposition temperature. $Ca(Ti, Fe)O_3$ began to form at 650 °C. The amount formed increased with deposition temperature up to 800 °C, at which an approximately isotropic $Ca(Ti, Fe)O_3$, corresponding to the JCPDS card of $CaTiO_3$ (Card no. 22–153), was identified. The deposited film was dark brown, which suggested the formation of solid-solution $Ca(Ti, Fe)O_3$. No other crystalline phase could be detected, which indicated the formation of a single phase of orthorhombic perovskite structure. However, the formation of $Ca(Ti, Fe)O_3$ was depressed at 900 °C, probably due to the thermal decomposition of organocomplexes of calcium or titanium before reaching the deposition zone. As a result, an excess amount of Fe_2O_3 (haematite) would be co-deposited. Fig. 5a–h show the XMA results which include the distribution maps of calcium, titanium and iron elements in the films deposited at 750 and 800 °C. The surface microstructural photographs are shown in Fig. 5a and b. Apparently, each element is homogeneously distributed in the whole film surface regardless of the film microstructure. An approximate composition of $Ca(Ti_{1-x}Fe_x)O_{3-\alpha}$ was estimated to be $x \sim 0.2$ in this specimen.

Fig. 6 shows the weight deposited and the film thickness of $Ca(Ti, Fe)O_3$ plotted against reaction time, where the deposition temperature is kept constant at 750 °C. The film thickness was measured by SEM observation. The deposition rate determined from the weight of the deposit decreases gradually with reaction time, which would be caused by a slight decrease in the amount of $Ca(DPM)_2$ evaporated with the passage of time. On the other hand, the film thickness curve has a shoulder up to about 60 min, when the deposition rate increases, probably on account of the change in the film-growth mechanism. Fig 7a–f are scanning electron micrographs which show a variation of microstructure of cross-sections and film surfaces with reaction time. A dense film with a thickness of 2.2 μm is prepared at a reaction time of 20 min, as seen in Fig. 7a and b. A columnar structure is formed by the grain growth of primary grains in the reaction time range of 40–60 min (see Fig. 7c and d). At the reaction time of 80–100 min (see Fig. 7e and f), however, secondary grains, which comprise aggregated primary grains, have grown to form a cone structure. Apertures can be observed among the secondary grains, which resulted in a decrease in the film density over the reaction time of 60 min, in accordance with the apparent increase in film thickness, as shown in Fig. 6.
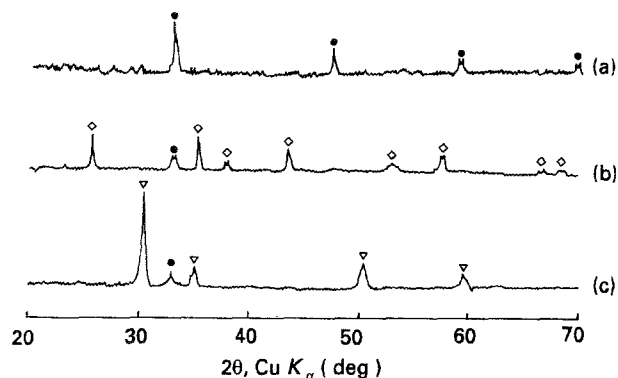

Figure 8 XRD patterns of the deposits on different substrates: (a) silica glass, (b) sintered Al_2O_3, (c) sintered ZrO_2–8 mol % Yb_2O_3. Deposition temperature 750 °C, reaction time 60 min, (●) $Ca(Ti, Fe)O_3$, (◇) Al_2O_3, (▽) ZrO_2–Yb_2O_3.
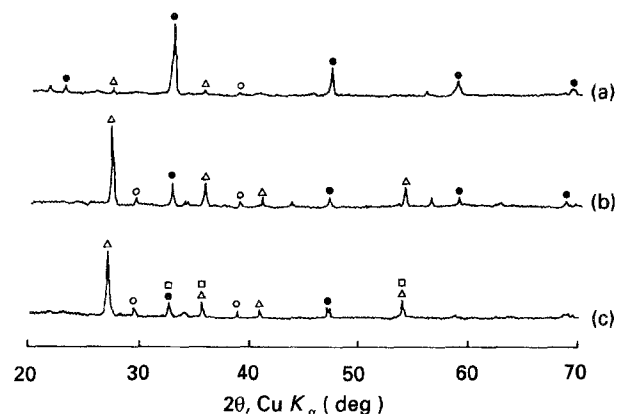

Figure 9 XRD patterns of the deposits on CVD oxide films on silica glass substrates: (a) CaO/silica glass, (b) TiO_2/silica glass, (c) Fe_2O_3/silica glass. Deposition temperature 750 °C, reaction time 60 min. (●) $Ca(Ti, Fe)O_3$, (△) TiO_2 (rutile), (○) $CaCO_3$, (□) Fe_2O_3 (haematite).

3.3. Influence of substrate material on the formation of Ca(Ti, Fe)O₃ film

Various substrates were used for the deposition of $Ca(Ti, Fe)O_3$ in order to examine the possibility of film formation on other kinds of substrates with rough or porous surface structures. A comparison of the deposited phases and morphologies was made of the products obtained on different substrate materials under the same optimum deposition conditions (deposition temperature 750 °C, reaction time 60 min). Fig. 8 shows the XRD patterns of deposits on some different substrates: (a) silica glass, (b) sintered Al_2O_3 and (c) sintered ytterbia (8 mol %)-stabilized zirconia. A uniform film of single-phase $Ca(Ti, Fe)O_3$ was obtained on silica glass substrate. The amount of $Ca(Ti, Fe)O_3$ formed was small, however, on both sintered compacts (b) and (c). The diffraction peaks of $Ca(Ti, Fe)O_3$ on a stabilized zirconia were especially weak. These data suggest that the formation of $Ca(Ti, Fe)O_3$ is greatly affected by the compositions or surface microstructures of the substrate materials used.

Fig. 9 shows the XRD patterns of the deposits obtained on the CVD-oxide films of metals (calcium,

titanium and iron) which are the metallic constituents of the target material $Ca(Ti, Fe)O_3$, Deposition experiments with $Ca(Ti, Fe)O_3$ were carried out immediately after the CVD run of each oxide film. On CaO/silica glass substrate, nearly a single phase of $Ca(Ti, Fe)O_3$ was formed in approximately the same amount as on silica glass substrate. However, the amount of $Ca(Ti, Fe)O_3$ formed decreased when using the substrates of TiO_2/silica glass or Fe_2O_3/silica glass, when non-perovskite oxide or carbonate were deposited instead. It is suggested from the above results that the calcium source tends to be deposited on to the SiO_2 or CaO with a certain chemical affinity.

On the other hand, it was found from the above experiments that the morphology of the deposits was influenced by the roughness of the substrate. For example, rather large grains of $Ca(Ti, Fe)O_3$ were easy to grow on a sintered compact, in which a uniform and dense film was relatively difficult to be formed. Further investigations will be necessary in order to obtain a dense film of $Ca(Ti, Fe)_3$ on a porous substrate.

4. Conclusions

A mixed conductor film of $Ca(Ti, Fe)O_3$ was prepared by a thermal decomposition CVD technique using organocomplexes as starting materials. The following conclusions were obtained through a series of experiments.

1. Three complexes were evaporated and transported nearly in a steady state at the evaporation temperatures of 245 °C for $Ca(DPM)_2$, 115 °C for $Fe(acac)_3$ and 45 °C for $Ti(O-C_3H_7)_4$ using a horizontal uniaxial reactor which comprised two evaporation furnaces for calcium and iron complexes and a deposition furnace.

2. A single phase of crystalline $Ca(Ti, Fe)O_3$ film was formed on silica glass substrate at the optimum deposition conditions: total nitrogen carrier gas flow rate 320 ml min^{-1}, oxygen flow rate 100 ml min^{-1}, total pressure 30 torr, deposition temperature 700–800 °C, and reaction time 20–60 min.

3. The amount of $Ca(Ti, Fe)O_3$ film formed and its microstructure were greatly affected by the composition and surface structure of the substrate materials. $Ca(DPM)$ in the vapour phase has a chemical affinity with SiO_2 or CaO substrate, which resulted in an increased amount of $Ca(Ti, Fe)O_3$ formed.

References

1. H. IWAHARA, *Petrotech*, **12** (1989) 224.
2. H. IWAHARA, T. ESAKA and T. MANGAHARA, *J. Appl. Electrochem.* **18** (1988) 173.
3. T. ESAKA, T. FUJII, K. SUWA and H. IWAHARA, *Solid State Ionics* **40/41** (1990) 544.
4. Y. SAKASHITA, T. ONO, H. SEGAWA, K. TOMINAGA and M. OKADA, *J. Appl. Phys.* **69** (1991) 8352.
5. H. FUNAKUBO, K. IMASHITA, N. KIEDA and N. MIZUTANI, *J. Ceram. Soc. Jpn* **99** (1991) 248.
6. H. FUNAKUBO, K. IMASHITA and N. MIZUTANI, *ibid.* **99** (1991) 1169.
7. H. NAKAZAWA, H. YAMANE and T. HIRAI, *ibid.* **99** (1991) 527.
8. M. de KEIJSER, G. J. M. DORMANS, J. F. M. CILLESSEN, D. M. de LEEUW and H. W. ZANDBERGEN, *Appl. Phys. Lett.* **58** (1991) 2636.
9. H. ZAMA and S. ODA, *Jpn J. Appl. Phys.* **29** (1990) L1072.
10. R. SINGH, S. SINHA, N. J. HSU, P. CHOU, R. K. SINGH and J. NARAYAN, *J. Appl. Phys.* **67** (1990) 1562.
11. N. HAMAGUCHI, J. VIGIL, R. GARDINER and P. S. KIRLIN, *Jpn J. Appl. Phys.* **29** (1990) L596.